

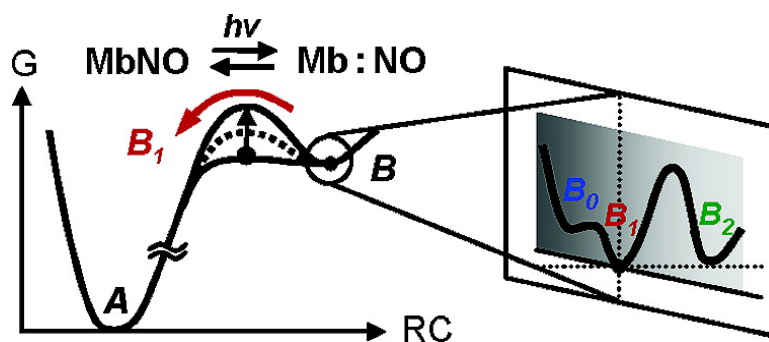
Communication

Protein Conformation-Induced Modulation of Ligand Binding Kinetics: A Femtosecond Mid-IR Study of Nitric Oxide Binding Trajectories in Myoglobin

Seongheun Kim, and Manho Lim

J. Am. Chem. Soc., **2005**, 127 (25), 8908-8909 • DOI: 10.1021/ja0502270 • Publication Date (Web): 01 June 2005

Downloaded from <http://pubs.acs.org> on March 25, 2009



More About This Article

Additional resources and features associated with this article are available within the HTML version:

- Supporting Information
- Links to the 2 articles that cite this article, as of the time of this article download
- Access to high resolution figures
- Links to articles and content related to this article
- Copyright permission to reproduce figures and/or text from this article

[View the Full Text HTML](#)

Protein Conformation-Induced Modulation of Ligand Binding Kinetics: A Femtosecond Mid-IR Study of Nitric Oxide Binding Trajectories in Myoglobin

Seongheun Kim and Manho Lim*

Department of Chemistry, Pusan National University, Busan 609-735, Korea

Received January 13, 2005; E-mail: mhlim@pusan.ac.kr

The rates of biochemical reactions in proteins are modulated by protein conformation. Myoglobin (Mb), a ligand-binding heme protein, has long served as a model system for investigating the dynamics of conformational change and the coupling of protein motions to ligand binding.¹ To unveil the mechanism of how protein conformational changes modulate ligand-binding reactions, it is most useful to characterize ligand-binding trajectories near the active site of the protein.

Time-resolved studies of photolyzed MbCO have revealed much about ligand-rebinding dynamics; however, under physiological conditions, the geminate rebinding (GR) yield is too small and its rate too low to characterize the extent to which protein conformational relaxation modulates the ligand-binding trajectories.² On the other hand, most of the photolyzed NO from MbNO geminately recombine within a few tens of picoseconds at room temperature,^{3–5} thereby allowing one to probe the effect of picosecond conformational relaxation on ligand binding. Strong coupling between the nuclear motion of the heme and NO rebinding reaction was reported.⁶ Early MD simulations on a series of Mb mutants suggested that NO rebinding is governed by constrained diffusion of NO in the heme pocket.⁷ The dynamics of NO rebinding were reported to be nonexponential,^{3–5} but the experimental methods used could not identify whether the complex rebinding character was a consequence of site heterogeneity, protein conformational relaxation, or both. To distinguish between these possible mechanisms, it is crucial to develop a site-specific probe of the ligand state.⁵ Here, we use femtosecond time-resolved IR spectroscopy to directly observe the photolyzed NO as it rebinds under physiological conditions. From these studies, the role of the protein conformation in modulating the geminate rebinding rate is determined unambiguously.

Figure 1 shows a series of time-resolved vibrational spectra in the “free” NO region after photolysis of MbNO in D₂O at 283 K.⁸ Since the spectral region probed is free from any protein absorption, and since each feature exhibits a ¹⁵NO isotopic shift, the features are assigned to NO and denoted as B states.⁹ The B states correspond to ligands photodissociated from the heme iron and remaining in the heme pocket. According to temperature-derivative spectroscopy of MbCO, multiple vibrational bands for the bound ligand (termed A states) arise from different protein structures (conformational substates, CS), and those for the photolyzed ligands result from different positions and/or orientations of the ligand within the heme pocket in a given CS.¹⁰ For the photolyzed ligand, the existence of CS gives rise to a distribution of band positions and yields a Gaussian band shape. The time-resolved spectra were modeled with a sum of three Gaussians (denoted B₀, B₁, and B₂)^{9,11} plus their red-shifted replicas, which arise from vibrationally excited NO. The positions of the bands shift, and their bandwidths shrink on the picosecond time scale. This spectral evolution, also observed in photolyzed CO spectra in Mb,¹² arises from conformational relaxation of Mb after photolysis. Conformational relaxation on this time scale has also been observed in the amide band¹³ and band

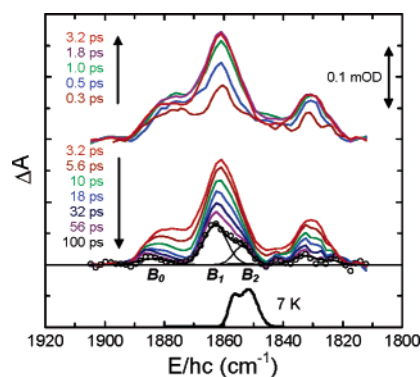


Figure 1. Time-resolved B state spectra of photolyzed MbNO. Data from 0.3 to 3.2 ps are offset to avoid overlap. The spectrum at 100 ps is decomposed into three Gaussian features labeled B₀, B₁, and B₂ plus a red-shifted replica of those features (O, data; —, fit). For comparison, the FTIR difference (photolyzed minus unphotolyzed) spectrum of ferrous MbNO at 7 K is shown (from ref 18).

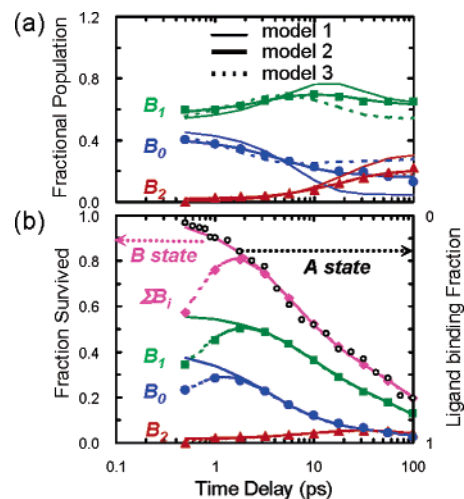
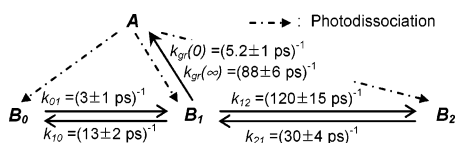


Figure 2. (a) Time dependence of the fractional B state population. The data are fitted to the three models described in the text. (b) Time dependence of the integrated B state absorbance and the A state bleach (O; from ref 8). The dotted lines represent the fit to the integrated absorbances using model 2 with an initial rise time, and the solid lines represent population of B states (see text).

III^{14,15} of photolyzed MbCO. The initial growth of the total integrated B state absorbance (Figure 2B), also observed in MbCO, has been attributed to structural reorganization of the neighboring protein residues surrounding the nascent docked ligand.¹² The population in each site is assumed to be proportional to its integrated absorbance.¹⁶ Time dependence of the integrated absorbance contains information about GR rates, transitions among B states, and the vibrational relaxation of excited NO. The integrated absorbance of each state was divided by the total integrated area to deduce the time-dependent fractional population of the B states

(Figure 2A). Interconversion between B states is manifested as time-dependent changes in the fractional population.

We have considered various models to describe the kinetic behavior of the B bands but have found only one acceptable model. Of those considered, three models are discussed in some detail. A kinetic model allowing parallel rebinding from all three B states and transitions between them could not fit the data (model 1, Figure 2A), demonstrating that the multiple-sites model, with time-independent rebinding rates, cannot explain the nonexponential NO rebinding. Since the most general kinetic scheme with *time-independent* rates cannot reproduce the data and transition rates between B states are suggested to be time-independent,¹⁷ rebinding rate is set to be time-dependent. A model incorporating a *time-dependent rebinding* from B₁ (model 2) is most consistent with the data. Recovered parameters from the global fit to whole spectra for the model 2 are as follows:¹⁹



The rise time of the integrated B state absorbance (0.6 ± 0.2 ps) is in reasonable agreement with that found in MbCO experiments ($1.1-1.6$ ps),¹² suggesting that the growth results from protein reorganization. Following the initial rise, the total population of photolyzed NO reproduces the time dependence of the integrated A states area (Figure 2B),⁸ confirming that B states indeed arise from photolyzed NO. The fit also recovers the initial partitioning of photolyzed NO ($41 \pm 6\%$ in B₀, $57 \pm 5\%$ in B₁, and $2 \pm 1\%$ in B₂).²⁰ Apparently, photolysis leads from A to mainly B₀ and B₁, B₁ thermally exchanges with B₀ and B₂, but NO rebinds primarily from B₁. These results are consistent with faster rebinding of B₁ than of B₂ at cryogenic temperature.¹⁸ The fact that the B₁ population is smaller than that of B₂ at 7 K suggests that a significant portion of B₁ has rebound, and B₁ and B₂ are kinetically trapped. This interpretation implies that at 7 K, the rebinding barrier is not fully established and is lower than the barriers to B state interconversion.⁸ The absence of B₀ at cryogenic temperatures¹⁸ may result from a rapid transition from B₀ to B₁.²¹ The recovered rate constant for the time-dependent change of the barrier height, $(16 \text{ ps})^{-1}$, is similar to the effective rate for conformational relaxation of Mb after photolysis, $(18 \text{ ps})^{-1}$.^{8,15}

A model allowing time-dependent rebinding from B₀ has also been used to fit the kinetics, but it severely deviates from the data (model 3), demonstrating that NO rebinds primarily via B₁.

A recent study using time-resolved polarized mid-IR spectroscopy²² showed that the orientational distribution of photolyzed CO in the heme pocket was consistent with an MD simulation in which CO was found to be confined within an L-shaped thin slab that contained two higher probability regions. It was suggested that B₁ and B₂ correlate with the $\sim 125^\circ$ and $\sim 90^\circ$ orientations found for the 1.3 and 2.3 Å (from the heme normal) high probability sites in the MD simulations, respectively.²² It was hypothesized that while B₁ and B₂ can interconvert freely under ambient conditions, ligand binding proceeds through B₁, the region nearer the heme iron.²² This hypothesis is well supported by our MbNO results. It also indicates that B₁ and B₂ are roto-isomers corresponding to photolyzed NO in adjacent sites in the heme pocket found in MD simulations.^{5,18,22}

Different conformational substates of bound MbNO have been found to exhibit the same GR kinetics.⁸ Here, we have shown that multiple sites with fixed barriers cannot reproduce the time-

dependent population of B states at room temperature. Consequently, a *time-dependent rebinding* barrier is required to reproduce the observed nonexponential rebinding dynamics. We conclude that a time-dependent barrier arising from protein relaxation on the same time scale as the rebinding process is responsible for the nonexponential rebinding. On the basis of this model, we show that photolysis leads to ultrafast translocation of NO to the heme pocket sites denoted B₀ and B₁, B₂ becomes thermally populated via B₁, and NO rebinds primarily via B₁.

Acknowledgment. This work was supported by grants from the KOSEF through CIMS (POSTECH).

Supporting Information Available: Experimental details, band assignment, and data analysis. This material is available free of charge via the Internet at <http://pubs.acs.org>.

References

- (1) Austin, R. H.; Beeson, K. W.; Eisenstein, L.; Frauenfelder, H.; Gunsalus, I. C. *Biochemistry* **1975**, *14*, 5355–5373. (b) Springer, B. A.; Sliagar, S. G.; Olson, J. S.; Phillips, G. N., Jr. *Chem. Rev.* **1994**, *94*, 699–714.
- (2) Henry, E. R.; Sommer, J. H.; Hofrichter, J.; Eaton, W. A. *J. Mol. Biol.* **1983**, *166*, 443–451.
- (3) Jongeward, K. A.; Magde, D.; Taube, D. J.; Marsters, J. C.; Traylor, T. G.; Sharma, V. S. *J. Am. Chem. Soc.* **1988**, *110*, 380–387.
- (4) Petrich, J. W.; Lambry, J. C.; Kuczera, K.; Karplus, M.; Poyart, C.; Martin, J. L. *Biochemistry* **1991**, *30*, 3975–3987.
- (5) Shreve, A. P.; Franzen, S.; Simpson, M. C.; Dyer, R. B. *J. Phys. Chem. B* **1999**, *103*, 7969–7975.
- (6) Zhu, L.; Sage, J. T.; Champion, P. M. *Science* **1994**, *266*, 629–632.
- (7) Li, H.; Elber, R.; Straub, J. E. *J. Biol. Chem.* **1993**, *268*, 17908–17916.
- (8) Kim, S.; Jin, G.; Lim, M. *J. Phys. Chem. B* **2004**, *108*, 20366–20375.
- (9) Alben, J. O.; Beece, D.; Bowne, S. F.; Doster, W.; Eisenstein, L.; Frauenfelder, H.; Good, D.; McDonald, J. D.; Marden, M. C.; Mo, P. P.; Reinisch, L.; Reynolds, A. H.; Shyamsunder, E.; Yue, K. T. *Proc. Natl. Acad. Sci. U.S.A.* **1982**, *79*, 3744–3748.
- (10) Mourant, J. R.; Braunstein, D. P.; Chu, K.; Frauenfelder, H.; Nienhaus, G. U.; Ormos, P.; Young, R. D. *Biophys. J.* **1993**, *65*, 1496–1507.
- (11) Lim, M.; Jackson, T. A.; Anfinrud, P. A. *J. Chem. Phys.* **1995**, *102*, 4355–4366.
- (12) (a) Lim, M.; Jackson, T. A.; Anfinrud, P. A. *Nat. Struct. Biol.* **1997**, *4*, 209–214. (b) Kim, S.; Heo, J.; Lim, M. *Bull. Korean Chem. Soc.* **2005**, *26*, 151–156.
- (13) Causgrove, T. P.; Dyer, R. B. *J. Phys. Chem.* **1996**, *100*, 3273–3277.
- (14) Kuczera, K.; Lambry, J. C.; Martin, J. L.; Karplus, M. *Proc. Natl. Acad. Sci. U.S.A.* **1993**, *90*, 5805–5807.
- (15) Lim, M.; Jackson, T. A.; Anfinrud, P. A. *Proc. Natl. Acad. Sci. U.S.A.* **1993**, *90*, 5801–5804.
- (16) The integrated absorbance of photolyzed NO is partitioned between the narrow B band and a broad unresolved pedestal.^{11,12} We assumed that the ratio of unresolved pedestal to the narrow band and time evolution of intensity into the narrow band are independent of the different B states.^{11,12,17}
- (17) Kim, S.; Lim, M. *J. Am. Chem. Soc.* **2005**, *127*, 5786–5787.
- (18) Miller, L. M.; Pedraza, A. J.; Chance, M. R. *Biochemistry* **1997**, *36*, 12199–12207.
- (19) Other transition rates were found to be too slow to be of any consequence and were set to 0. The transition rate from B_i to B_j is denoted k_{ij} . The time-dependent rebinding rate, $k_{gr}(t)$, was modeled in the same way to fit the A state bleach recovery kinetics.^{4,8} The fitted parameters are: $A = 2 \times 10^{11} \text{ s}^{-1}$; $k_{\text{bar}} = (16 \text{ ps})^{-1}$; $E_0 = 0.027 \text{ kcal/mol}$; and $E_{\text{eq}} = 1.6 \text{ kcal/mol}$. If the oscillator strength of the B state changes with 400 fs time scale, as reported,²³ the recovered fast time constant may have higher uncertainty. The free induction decay of the spectrum lasting ~ 1 ps can also add uncertainty to k_{01} .
- (20) The nascent distribution of NO will be dictated by energetics of the departing ligand, which is related to the pump wavelength.
- (21) One prominent difference between photolyzed NO and CO is the absence of B₀ in MbCO at ambient temperature.^{9,11} The blue-shifted B₀ band likely arises from a H bond between the N atom of NO with the distal histidine.²⁴ While CO forms a H bond in only linear or slightly bent geometries, NO can form a H bond in a severely bent geometry, with the most stable H bond formed at $\angle(\text{HNO}) = \sim 130^\circ$.²⁴ The proximity and orientation of “docked” CO may allow only a weak H bond, resulting in no measurable B₀ band for CO at room temperature. The rapid transition between B₀ and B₁ suggests that B₀ is located very close to B₁.
- (22) Lim, M.; Jackson, T. A.; Anfinrud, P. A. *J. Am. Chem. Soc.* **2004**, *126*, 7946–7957.
- (23) Polack, T.; Ogilvie, J. P.; Franzen, S.; Vos, M. H.; Joffe, M.; Martin, J. L.; Alexandrou, A. *Phys. Rev. Lett.* **2004**, *93*, 018102/1–018102/4.
- (24) (a) Krim, L.; Alikhani, M. E. *Chem. Phys.* **1998**, *237*, 265–271. (b) Rensberger, K. J.; Blair, J. T.; Weinhold, F.; Crim, F. F. *J. Chem. Phys.* **1989**, *91*, 1688–1696.

JA0502270